

SCIENTIFIC REPORTS



OPEN

Discovery and characterization of functional modules associated with body weight in broilers

Eirini Tarsani¹, Andreas Kranis^{2,3}, Gerasimos Maniatis², Santiago Avendano², Ariadne L. Hager-Theodorides¹ & Antonios Kominakis¹

Aim of the present study was to investigate whether body weight (BW) in broilers is associated with functional modular genes. To this end, first a GWAS for BW was conducted using 6,598 broilers and the high density SNP array. The next step was to search for positional candidate genes and QTLs within strong LD genomic regions around the significant SNPs. Using all positional candidate genes, a network was then constructed and community structure analysis was performed. Finally, functional enrichment analysis was applied to infer the functional relevance of modular genes. A total number of 645 positional candidate genes were identified in strong LD genomic regions around 11 genome-wide significant markers. 428 of the positional candidate genes were located within growth related QTLs. Community structure analysis detected 5 modules while functional enrichment analysis showed that 52 modular genes participated in developmental processes such as skeletal system development. An additional number of 14 modular genes (*GABRG1*, *NGF*, *APOBEC2*, *STAT5B*, *STAT3*, *SMAD4*, *MED1*, *CACNB1*, *SLAIN2*, *LEMD2*, *ZC3H18*, *TMEM132D*, *FRYL* and *SGCB*) were also identified as related to body weight. Taken together, current results suggested a total number of 66 genes as most plausible functional candidates for the trait examined.

Body weight (BW) is an economically important trait for the broiler industry. This trait also presents considerable biological interest as it is a typical complex (polygenic) trait. To date, the ChickenQTLdb¹ contains over 7,812 QTL/SNP associations of which 3,582 are related to growth. Several genome wide association studies (GWAS) have already been performed for growth traits (e.g.^{2,3}) in the species. The development of the chicken 600k SNP array⁴ facilitates efficient screening for causal loci and genes with relevance to target traits due to the uniform coverage across chromosomes and the inclusion of markers within coding regions. Despite the large number of findings by GWAS, understanding of the genetic architecture of BW in chicken remains limited⁵, since only a small number of positional candidate genes are confirmed as truly functionally relevant to the trait (e.g. *HDAC2* and *GNPDA2*^{6,7}). The use of various Bioinformatics tools such as gene enrichment analysis⁸, pathway analysis⁹ and gene network analysis¹⁰ can tackle this problem and aid in identifying the most promising functional candidate genes for the trait under study. Moreover, applications such as GeneMANIA¹¹ that is based on the guilt-by-association (GBA) principle¹² may also facilitate the identification of true causative genetic variants. The GBA principle states that gene products, which are protein interaction partners, tend to be functionally related¹³. Furthermore, genes in protein–protein interaction networks (PPINs) are organized into densely linked clusters i.e. communities or modules¹⁴. Modules present a structurally independent gene sub-network with more interior connections and consist of proteins which have the same or similar biological function(s)¹⁵. Modules could be further distinguished in protein complexes and in dynamic functional modules. Protein complexes are formed by several proteins which interact at the same place and time while dynamic functional modules are composed of few proteins participating in a specific cellular function not necessarily at the same place and time¹⁶. Moreover, functional modules consist of one or multiple protein complexes participating in a common biological process¹⁷. Since modules do not emerge by chance, they can reveal interactions with biological importance within large PPINs^{16,18}. The module-based approach has already been used to cluster genes into functional groups and to predict protein functions¹⁹. Investigation of functional modules has mainly been focused on human diseases such as

¹Department of Animal Science and Aquaculture, Agricultural University of Athens, Iera Odos 75, 11855, Athens, Greece. ²Aviagen Ltd., Newbridge, Midlothian, EH28 8SZ, UK. ³The Roslin Institute, University of Edinburgh, EH25 9RG, Midlothian, United Kingdom. Correspondence and requests for materials should be addressed to E.T. (email: etarsani@aia.gr)

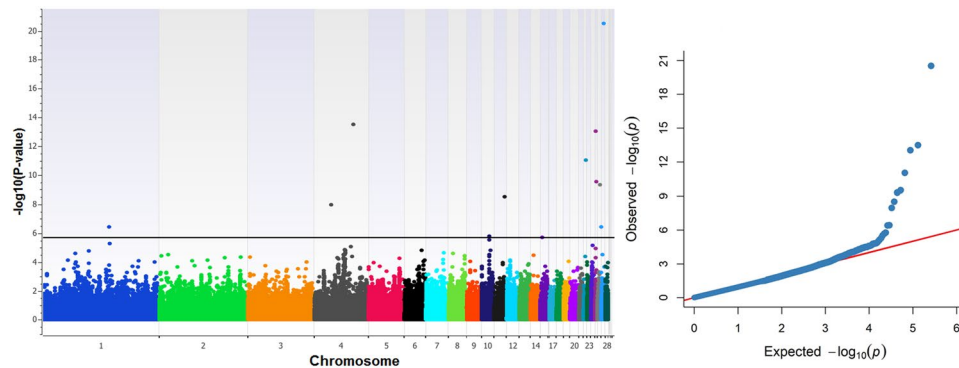


Figure 1. Manhattan plot (left) and quantile-quantile plot (right) for BW. Manhattan plot shows the $-\log_{10}$ (observed p-values) of the genome-wide SNPs (y-axis) across the 28 autosomes (x-axis), and the horizontal line denotes the genome-wide significant threshold. With regard to the Q-Q plot, the y-axis represents the observed $-\log_{10}$ (p-values) and the x-axis shows the expected $-\log_{10}$ (p-values). Manhattan plot was constructed with SNP & Variation Suite (version 8.8.1) software (Golden Helix: <http://www.goldenhelix.com>) while Q-Q plot with the CMplot package (<https://github.com/YinLiLin/R-CMplot>) in R (<http://www.r-project.org/>).

SNP ID	GGA	Position (bp) ¹	$-\log_{10}$ (p-value)	FDR p-value
rs13923872	1	112,741,685	6.415	0.0112
rs312691174	4	29,074,989	7.948	0.00037
rs15608447	4	66,885,210	13.489	4.25E-09
rs318199727	10	13,536,548	5.763	0.04111
rs318098582	11	18,651,449	8.513	0.00012
rs317945754	15	3,557,083	5.677	0.04594
rs316794400	22	4,594,855	11.033	6.07E-07
rs317288536	25	976,833	13.035	8.05E-09
rs312758346	25	2,412,866	9.517	1.59E-05
rs317627533	26	4,597,439	9.313	2.12E-05
rs314452928	27	104,022	6.398	0.0105
rs315329074	27	4,528,275	20.513	8.05E-16

Table 1. Genome-wide significant SNPs (FDR p-value < 0.05) for BW. ¹Positions are based on *Gallus gallus*-5.0 genome assembly.

obesity²⁰, breast cancer^{21,22}, coronary artery disease²³ and asthma²⁴. Apart from human, functional modules have been identified in other species as well, such as in *Mus musculus* for discrete and rhythmic forelimb movements in motor cortex²⁵ and in *Gallus gallus* for muscle development and intramuscular fat accumulation at different post-hatching ages²⁶.

Driven from findings in other species and traits, aim of the present study was first to investigate whether body weight in broilers is associated with functional modules and second to propose novel candidate genes for the trait in question.

Results

Significant SNPs and positional candidate genes. Figure 1 shows the Q-Q plot of the expected and the observed p values ($-\log_{10}$ p values) of all SNPs. The genomic inflation factor (λ) was also estimated as high as 0.93. According to Kang *et al.*²⁷, λ values that lie outside of the conservative 95% confidence interval (0.992 to 1.008) denote dependency of SNPs. However, as the Q-Q plot clearly shows, there is no evidence of any systematic bias due to population structure or analytical approach in our case. As Yang *et al.*²⁸ emphasize in their paper, it is reasonable to expect deviation(s) of λ from 1 for purely polygenic traits such as that examined here in the absence of any systematic bias. The Q-Q plot also shows that some SNPs depart from the expected probability and thus might be associated with the trait. These SNPs are also displayed in Fig. 1 in a form of a Manhattan plot.

Specifically, there were 12 SNPs detected, across nine autosomes (1, 4, 10, 11, 15, 22, 25, 26 and 27) reaching genome-wide significance (FDR p-value < 0.05). A detailed description of the significant (lead) SNPs is provided in Table 1. Table 2 displays the extent of genomic regions displaying strong LD ($D' > 0.8$) around the lead markers that were searched for positional candidate genes. Note that marker rs312758346 (GGA25) was omitted here as LD levels around this marker were below the threshold LD value ($D' < 0.8$). In total, 645 positional candidate genes were identified within the searched genomic regions (Supplementary Table S1). From the candidate genes, n = 15 were microRNAs with 13 of them (*MIR6672*, *MIR1720*, *MIR7-2*, *MIR3529*, *MIR1571*, *MIR1560*, *MIR1785*, *MIR6662*, *MIR7454*, *MIR10A*, *MIR6663*, *MIR1735* and *MIR6547*) published in the miRBase database (<http://>

SNP ID	GGA	Position (bp) ¹	Searched genomic range around 'lead' SNP (\pm bp)	D'	Number of positional candidate genes	Number of QTL/associations
rs13923872	1	112,741,685	613,054	0.91	33	20
rs312691174	4	29,074,989	650,472	1	16	14
rs15608447	4	66,885,210	718,407	0.88	36	36
rs318199727	10	13,536,548	737,906	0.83	33	11
rs318098582	11	18,651,449	300,257	0.81	27	9
rs317945754	15	3,557,083	935,183	0.99	20	21
rs316794400	22	4,594,855	26,589	0.96	7	1
rs317288536	25	976,833	1,004,513	0.83	176	—
rs317627533	26	4,597,439	773,988	0.9	93	6
rs314452928	27	104,022	140,067	0.94	12	3
rs315329074	27	4,528,275	998,553	0.98	192	65

Table 2. Number of positional candidate genes and QTL/associations within the searched genomic regions (\pm maximum distance of the farthest SNP being in strong LD ($D' > 0.8$) with the lead SNP; D' : average D' values within the searched genomic region). ¹Positions are based on *Gallus gallus*-5.0 genome assembly.

www.mirbase.org/) for the species. Moreover, 190 candidate genes were unannotated (LOC) resulting in a total number of 455 annotated positional candidate genes. The maximum number of candidate genes ($n = 192$) was identified in a region spanning 998.5 kb (average $D' = 0.98$) around marker *rs315329074* on GGA27. At the other extreme, the smallest number of candidate genes was identified for *rs316794400* within a narrow region spanning 26.6 kb (average $D' = 0.96$) on GGA22. Six out of the 11 lead markers were located within annotated genes i.e. *SLAIN2* (GGA4), *ZC3H18* (GGA11), *TMEM132D* (GGA15), *F-KER* (GGA25), *LEMD2* (GGA26) and *CACNB1* (GGA27).

Reported QTL/associations. Table 2 shows the number of published QTL/associations reported within the searched genomic regions. A total of 186 QTL/associations related to growth traits or carcass traits (carcass weight, abdominal fat percentage, breast muscle percentage and average daily gain) were identified within the searched regions. QTL/associations were distributed across eight chromosomes (1, 4, 10, 11, 15, 22, 26 and 27) and a detailed description of the reported QTL can be found in Supplementary Table S2. Note that the searched region around *rs317288536* (GGA25) is not reported to harbor any QTL/association (Table 2). Furthermore, the only QTL reported on GGA22 as well as two additional QTL on GGA26 and GGA27 could not be remapped in *Gallus gallus*-5.0 by the Genome remapping service tool from NCBI database. Nevertheless, based on the *Gallus gallus*-4 genome assembly, the searched regions around *rs316794400*, *rs317627533* and *rs314452928* overlapped with three QTL (IDs: 95429, 30883 and 55944). The maximum number ($n = 65$) of QTL/associations was reported around *rs315329074* (GGA27) and the minimum number ($n = 1$) around *rs316794400* (GGA22). Nine out of the 12 lead SNPs on autosomes 1, 4, 10, 11, 15, 26 and 27 lie within 96 out of the 186 growth-related QTL (Supplementary Table S2). In addition, nearly all reported QTL on the searched regions on GGA4 ($n = 49/50$) and GGA11 ($n = 9/9$) contain at least one of the lead markers (*rs312691174*, *rs15608447* and *rs318098582* respectively).

We further sought to examine the locations of the positional candidate genes in the relation to the positions of the reported QTL. These results are illustrated in Fig. 2 in forms of circular maps for seven autosomes (1, 4, 10, 11, 15, 26 and 27). On GGA1, all 33 candidate genes (around *rs13923872*) are lying in a genomic region spanning from 2421 to 196203 kb where 17 relevant QTL have been reported. On GGA4, all 16 candidate genes around *rs312691174* are located within a region spanning from 4965 to 91268 kb, where all 14 published QTL reside. On the same autosome, all genes ($n = 36$) around the second significant marker (*rs15608447*) are located in a region spanning from 4965 to 91268 kb where 35 QTL relevant to body weight, liver weight, carcass weight, total white fat weight have been reported. On GGA10, the region spanning from 693 to 20423 kb around the 'lead' marker (*rs318199727*) harbours all the 33 candidate genes and overlaps with 6 growth related QTL. On GGA11, in a region spanning from 953 to 20209 kb around *rs318098582* there have been 7 reported QTL and 27 candidate genes identified. On GGA15, in a region spanning from 1932 to 10689 kb around *rs317945754*, 6 QTL related to growth traits (visceral fat weight, abdominal fat weight and breast muscle weight) are reported and 20 candidate genes were identified. Moreover, on GGA26 (*rs317627533*), 64 out of the 93 candidate genes lie in a narrow region (1264 to 4918 kb) where QTL associated with growth traits such as body weight and shank weight, are reported. On GGA27 in a regions spanning from 55 to 4520 kb around *rs314452928*, 2 related QTL were identified including 7 out of the 12 candidate genes. All 192 genes around the second marker (*rs315329074*) on GGA27 were located within one published QTL spanning 3788 to 5630 kb that has been associated with thigh percentage. In total, 428 out of the 462 positional candidate genes (genes on GGA22 and GGA25 were not included here) were located within regions with reported QTL/associations.

Detection of community structure. A network including 402 genes (nodes) and 5294 interactions (edges) was generated. Note that for *APOA1BP* and *LOH11CR2A* genes the homologous human gene descriptions (*NAXE* and *VWA5A*) were used, respectively. Community structure analysis detected 5 modules, formed by 401 genes (see Supplementary Table S3). One more module was also detected but this was consisted by only

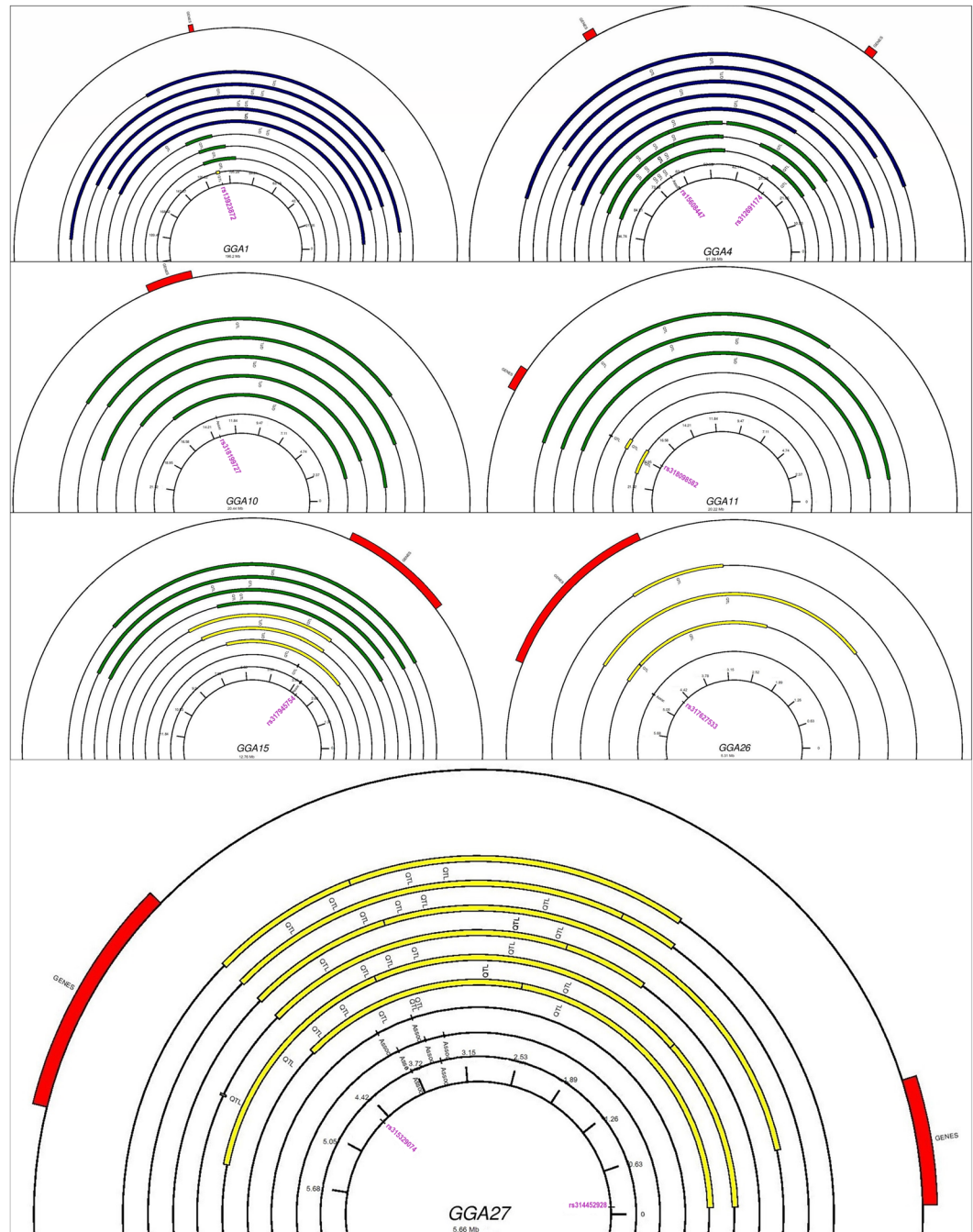


Figure 2. Circular chromosome maps for seven autosomes presenting combined data of reported QTL ($n = 183$) and positional candidate genes ($n = 462$). Blue color represents the extent of large sized QTL (50–196.2 Mb), green color the medium sized QTL (5–50 Mb) and the yellow color is indicative of the small QTL (0–5 Mb). Red color indicates the starting and ending positions of positional candidate genes. The position(s) of the significant SNPs (labeled in purple color) is also given. The figure was constructed using GenomeVx⁸⁷.

one gene (*NIPAL1*). Thus it cannot be considered as a typical module. Note that this gene network had a strong community structure as indicated by the high (0.59) estimated modularity value²⁹. Distribution of the 401 genes across the 5 modules is displayed in Fig. 3. Module_2 consisted of 187 genes, module_3 of 22 genes, module_4 of 18 genes, module_5 of 152 genes and module_6 of 22 genes.

Functional enrichment analysis per module. Four (module_ID: 2–5) out of the five modules exhibited enriched GO BPs while only three modules were associated with developmental processes according to QuickGO. Specifically, in module_2, a total number of 21 enriched GO BPs (Supplementary Table S4) and 78 participating genes were identified. According to QuickGO (see Figs 3 and 4), 9 out of the 21 GO BPs were related to development with 42 member genes (Supplementary Table S4). In the same module, 8 genes belonging to the

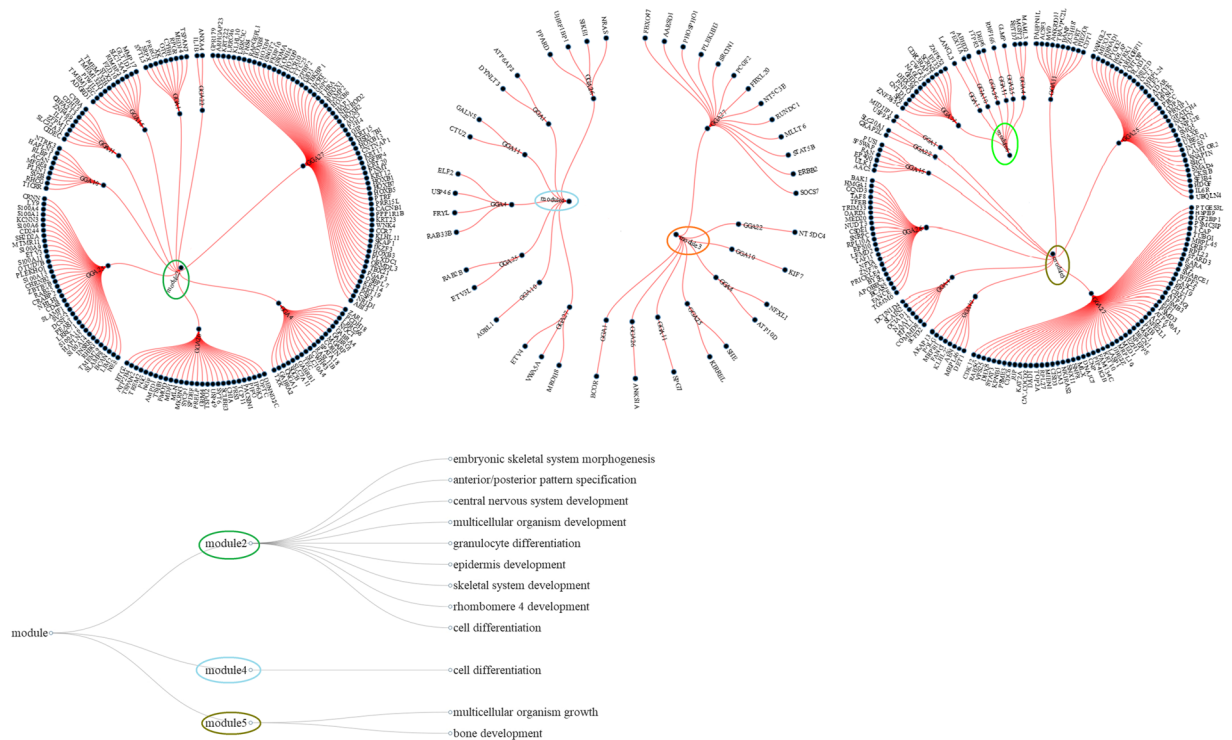


Figure 3. Network modules along with the significantly enriched developmental processes per module. The five modules are presented in the three radial networks (on the top) as circles/ellipses with different color together with their member genes and the corresponding chromosomes. The diagonal network at the bottom provides the significantly enriched developmental processes per module. Figure was constructed using the data.tree and networkD3 packages in R (<http://www.r-project.org/>).

homeobox B family genes along with *MDFI* were found to be enriched in embryonic skeletal system morphogenesis (GO:0048704). In module_3, none of the enriched GO BP terms were related to development (Supplementary Table S4). In module_4, three significantly enriched BPs (Supplementary Table S4) were identified in 7 member genes. Here, the only GO BP term that was associated with development through QuickGO was cell differentiation (GO:0030154) with 4 member genes (*PPARD*, *ELF2*, *ETV3L* and *ETV4*, Fig. 4). A total number of 29 GO BPs were found as significantly enriched in module_5 (Supplementary Table S4). Here, two development related processes i.e. multicellular organism growth (GO:0035264) and bone development (GO:0060348) were identified by QuickGO (Fig. 4) with 6 involved genes (*KAT2A*, *SP2*, *ANKRD11*, *RARA*, *BGLAP* and *AKAP13*).

Functional candidate genes. An exhaustive list, including 66 modular genes, of the most plausible candidate genes for BW is provided in Table 3. From these genes, 52 were participating in enriched developmental processes, 7 were growth related genes that were not enriched to any developmental process and 7 were growth related genes identified in previous studies. These 66 modular genes were distributed across 7 chromosomes (GGA4, GGA10, GGA11, GGA15, GGA25, GGA26 and GGA27) with 47 of them detected in module_2. The *KRT* (keratins) family and B cluster of *HOX* (homeobox) family genes were also included here.

Discussion

Results of the present study have shown that a typical quantitative trait such as that examined here is associated with modular genes exhibiting functional relevance to developmental processes. This means that application of functional enrichment analysis on modular genes can facilitate the identification of true causative genes for the trait under study. Following this approach, a total number of 52 functional candidate genes could be identified in the present study. Example genes that fall in this category were the following: *BTG2*, *ZAR1*, *MEOX1*, *KRT14*, *KRT15*, *TXK*, *CSF3*, *ACAN*, *HOXB*, *MDFI*, *NES*, *IGFBP4*, *PRELP*, *PPARD*, *ELF2*, *KAT2A*, *RARA* and *BGLAP*. Specifically, *BTG2*, *ZAR1*, *MEOX1*, *KRT14* and *KRT15* have been reported to participate in cerebellar development³⁰, development of follicular oocytes³¹, somite differentiation³², keratinocytes proliferation³³ and pigmentation of muscle tissues³⁴, in chickens, respectively. *TXK* (*TXK tyrosine kinase*) has been reported as BW related gene³⁵ while *CSF3* (*colony stimulating factor 3*) has been described as a myelomonocytic growth factor in the species³⁶. *ACAN* (*aggrecan*) is essential for cartilage formation during development in chicken and mouse mutants³⁷ and the *HOX B* cluster genes are expressed in chick embryonic development³⁸. The *MDFI* (*MyoD family inhibitor*) tumor suppressor gene is known to have a negative effect on myogenic regulatory factors³⁹ while *NES* (*nestin*) is known as a neural progenitor cell marker during central nervous system development and a marker protein for neovascularization⁴⁰. Furthermore, *IGFBP4* (*insulin like growth factor binding protein 4*) is required for the

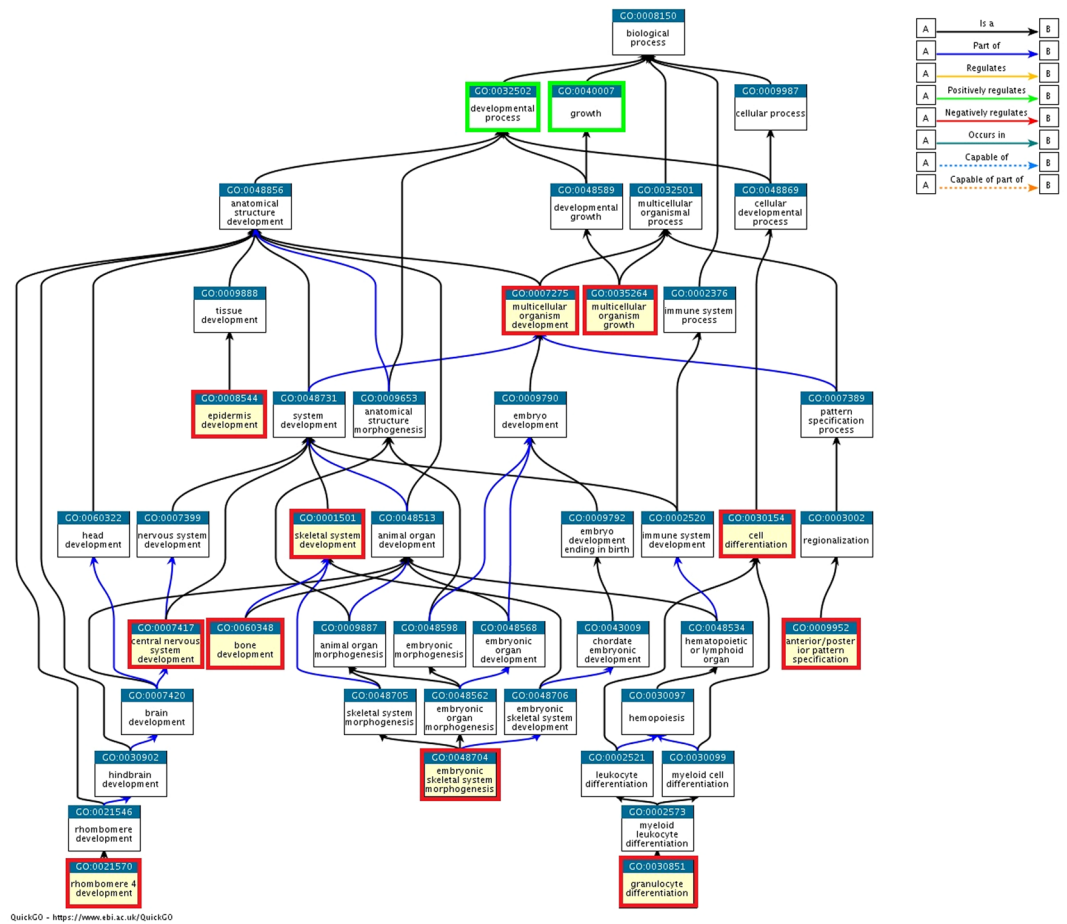


Figure 4. GO hierarchical structure for the eleven significantly enriched BPs (denoted with red color) associated with developmental process/growth term (denoted with green color). This GO tree was created and extracted by QuickGO⁸⁶.

adipose tissue development⁴¹ while *PRELP* (proline and arginine rich end leucine rich repeat protein) is highly expressed in cartilage, basement membranes, and bone development⁴². *PPARD* (peroxisome proliferator activated receptor delta) is a critical gene for normal adipose development and lipid homeostasis⁴³ while *ELF2* (*E74 like ETS transcription factor 2*) plays a key role in the development of lymphocytes⁴⁴. *KAT2A* (lysine acetyltransferase 2A) is necessary for growth and differentiation of craniofacial cartilage and bone in zebrafish and mice⁴⁵, *RARA* (retinoic acid receptor alpha) affects the hippocampal development⁴⁶ and finally *BGLAP* is produced by osteoblasts shaping new bones in chickens⁴⁷.

However, the search for modular genes that are exclusively enriched in functionally relevant terms has not proved to be efficient in identifying all true functional candidate genes. This finding may be fairly supported by the fact that 7 more genes (*GABRG1*, *NGF*, *APOBEC2*, *STAT5B*, *STAT3*, *SMAD4* and *MED1*) that despite having well documented relevance to development were found to be enriched in other but developmental GO BP terms. Specifically, *GABRG1* (gamma-aminobutyric acid type A receptor gamma 1 subunit) is reported as a BW related gene³⁵ and *NGF* (nerve growth factor) is a regulator of the somite survival and axial rotation during early chicken embryo development⁴⁸. *APOBEC2* (apolipoprotein B mRNA editing enzyme catalytic subunit 2) is known as a critical regulator and maintainer of muscle development in mammals and might affect muscle development in chickens⁴⁹. In the species, *STAT5B* (signal transducer and activator of transcription 5B) is associated with growth⁵⁰. *STAT3* (signal transducer and activator of transcription 3) plays a central role in development⁵¹. *SMAD4* (*SMAD family member 4*) is a central mediator of the transforming growth factor β signaling pathway which affects among others the cell growth⁵² and finally *MED1* (mediator complex subunit 1) has a key role in mammary epithelial cell growth⁵³.

The list with the most plausible candidate genes for the trait was, however, not exhausted in the previous two categories since 7 more genes (*CACNB1*, *SLAIN2*, *LEMD2*, *ZC3H18*, *TMEM132D*, *FRYL* and *SGCB*) with well documented implication to BW, were completely omitted in any enrichment analysis. Most interestingly, five of the above genes (*CACNB1*, *SLAIN2*, *LEMD2*, *ZC3H18* and *TMEM132D*) contained lead SNPs. *CACNB1* (calcium voltage-gated channel auxiliary subunit beta 1) has been reported to affect skeletal muscle development⁵⁴ in mice. *SLAIN2* (*SLAIN motif family member 2*) is necessary for the normal structure of microtubule cytoskeleton as it controls the microtubule growth during interphase⁵⁵. *LEMD2* (*LEM domain containing 2*) participates in nuclear structure organization⁵⁶ and plays an important role in mouse embryonic development by regulating various

Criterion	Gene	Description	Module_ID	GGA
modular genes participating in enriched developmental processes	<i>BTG2</i>	<i>BTG anti-proliferation factor 2</i>	module_2	26
	<i>ZAR1</i>	<i>zygote arrest 1</i>	module_2	4
	<i>MEOX1</i>	<i>mesenchyme homeobox 1</i>	module_2	27
	<i>KRT14</i>	<i>keratin 14</i>	module_2	27
	<i>KRT15</i>	<i>keratin 15</i>	module_2	27
	<i>TXK</i>	<i>TXK tyrosine kinase</i>	module_2	4
	<i>CSF3</i>	<i>colony stimulating factor 3</i>	module_2	27
	<i>ACAN</i>	<i>aggrecan</i>	module_2	10
	<i>HOXB1</i>	<i>homeobox B1</i>	module_2	27
	<i>HOXB2</i>	<i>homeobox B2</i>	module_2	27
	<i>HOXB3</i>	<i>homeobox B3</i>	module_2	27
	<i>HOXB4</i>	<i>homeobox B4</i>	module_2	27
	<i>HOXB5</i>	<i>homeobox B5</i>	module_2	27
	<i>HOXB6</i>	<i>homeobox B6</i>	module_2	27
	<i>HOXB7</i>	<i>homeobox B7</i>	module_2	27
	<i>HOXB8</i>	<i>homeobox B8</i>	module_2	27
	<i>HOXB9</i>	<i>homeobox B9</i>	module_2	27
	<i>HOXB13</i>	<i>homeobox B13</i>	module_2	27
	<i>MDFI</i>	<i>MyoD family inhibitor</i>	module_2	26
	<i>NES</i>	<i>nestin</i>	module_2	25
	<i>TBX21</i>	<i>T-box 21</i>	module_2	27
	<i>IGFBP4</i>	<i>insulin like growth factor binding protein 4</i>	module_2	27
	<i>PRELP</i>	<i>proline and arginine rich end leucine rich repeat protein</i>	module_2	26
	<i>HAPLN2</i>	<i>hyaluronan and proteoglycan link protein 2</i>	module_2	25
	<i>HAPLN3</i>	<i>hyaluronan and proteoglycan link protein 3</i>	module_2	10
	<i>GABRA4</i>	<i>gamma-aminobutyric acid type A receptor alpha4 subunit</i>	module_2	4
	<i>BCAN</i>	<i>brevican</i>	module_2	25
	<i>NHLH1</i>	<i>nescient helix-loop-helix 1</i>	module_2	25
	<i>ZBTB7B</i>	<i>zinc finger and BTB domain containing 7B</i>	module_2	25
	<i>FZD10</i>	<i>frizzled class receptor 10</i>	module_2	15
	<i>TCP11</i>	<i>t-complex 11</i>	module_2	26
	<i>PIWIL1</i>	<i>piwi like RNA-mediated gene silencing 1</i>	module_2	15
	<i>SPDEF</i>	<i>SAM pointed domain containing ETS transcription factor</i>	module_2	26
	<i>ZFPM1</i>	<i>zinc finger protein, FOG family member 1</i>	module_2	11
	<i>CBFA2T3</i>	<i>CBFA2/RUNX1 translocation partner 3</i>	module_2	11
	<i>KRT17</i>	<i>keratin 17</i>	module_2	27
	<i>CRABP2</i>	<i>cellular retinoic acid binding protein 2</i>	module_2	25
	<i>SH2D2A</i>	<i>SH2 domain containing 2A</i>	module_2	25
	<i>NR1D1</i>	<i>nuclear receptor subfamily 1 group D member 1</i>	module_2	27
	<i>STX2</i>	<i>syntaxin 2</i>	module_2	15
	<i>TEC</i>	<i>tec protein tyrosine kinase</i>	module_2	4
<i>ETV3</i>	<i>ETS variant 3</i>	module_2	25	
<i>PPARD</i>	<i>peroxisome proliferator activated receptor delta</i>	module_4	26	
<i>ELF2</i>	<i>E74 like ETS transcription factor 2</i>	module_4	4	
<i>ETV3L</i>	<i>ETS variant 3 like</i>	module_4	25	
<i>ETV4</i>	<i>ETS variant 4</i>	module_4	27	
<i>KAT2A</i>	<i>lysine acetyltransferase 2A</i>	module_5	27	
<i>RARA</i>	<i>retinoic acid receptor alpha</i>	module_5	27	
<i>BGLAP</i>	<i>bone gamma-carboxyglutamate protein</i>	module_5	25	
<i>SP2</i>	<i>Sp2 transcription factor</i>	module_5	27	
<i>ANKRD11</i>	<i>ankyrin repeat domain 11</i>	module_5	11	
<i>AKAP13</i>	<i>A-kinase anchoring protein 13</i>	module_5	10	
growth related modular genes not significantly enriched to any developmental process	<i>GABRG1</i>	<i>gamma-aminobutyric acid type A receptor gamma1 subunit</i>	module_2	4
	<i>NGF</i>	<i>nerve growth factor</i>	module_2	26
	<i>APOBEC2</i>	<i>apolipoprotein B mRNA editing enzyme catalytic subunit 2</i>	module_5	26
Continued				

Criterion	Gene	Description	Module_ID	GGA
	STAT5B	signal transducer and activator of transcription 5B	module_3	27
	STAT3	signal transducer and activator of transcription 3	module_5	27
	SMAD4	SMAD family member 4	module_5	25
	MED1	mediator complex subunit 1	module_5	27
growth related modular genes reported in previous studies	CACNB1	calcium voltage-gated channel auxiliary subunit beta 1	module_2	27
	SLAIN2	SLAIN motif family member 2	module_5	4
	LEMD2	LEM domain containing 2	module_5	26
	ZC3H18	zinc finger CCCH-type containing 18	module_5	11
	TMEM132D	transmembrane protein 132D	module_2	15
	FRYL	FRY like transcription coactivator	module_4	4
	SGCB	sarcoglycan beta	module_2	4

Table 3. List of 66 most plausible candidate genes for BW according to the following criteria: modular genes participating in enriched developmental processes, growth related modular genes not significantly enriched to any developmental process and growth related modular genes reported in previous studies.

signaling pathways such as MAPK (mitogen-activated protein kinase) and AKT (also known as Protein Kinase B)⁵⁷. *ZC3H18* (zinc finger CCCH-type containing 18) participates in RNA degradation⁵⁸ and affects mRNA metabolism⁵⁹. Finally, *TMEM132D* (transmembrane protein 132D) may function as a tumor suppressor gene⁶⁰. Finally, both *FRYL* (*FRY* like transcription coactivator) and *SGCB* (*sarcoglycan beta*) have been associated with growth^{61,62} in the species.

The two aforementioned gene lists underline the potential limitations of a cluster based method such as that used here to assess the biological properties of the candidate gene sets. Specifically, these limitations relate to i) grouping of similar terms into a cluster and evaluating the enrichment of functional clusters instead of each individual term within the clusters and ii) the evaluation of the identified term clusters separately, while not taken into consideration the relationships between clusters⁶³.

Apart from functional enrichment analysis, other analyses such as pathway analysis, gene network analysis and GBA gene prioritization analysis could also assist in identifying true causative genetic variants for the trait under study. For instance, in a previous study⁶⁴, the use of GBA gene prioritization analysis on 1,012 positional candidate genes revealed 248 functional candidate genes for the same trait. However, fixed genomic regions (of 1 Mb) around the lead genomic markers were used in that study. A final interesting result of the present study was the discovery of 15 microRNAs within the 645 candidate genes for the trait under investigation. One of these, i.e. *MIR10A* has been reported as significant for feed intake in broilers⁶⁵. *MIR10A* together with *MIR10B* have been reported to inhibit the development of human, mouse and rat granulosa cells during folliculogenesis⁶⁶. Finally, *MIR7-2* has been reported as genomic locus for peroxisome proliferator activated receptor regulation⁶⁷ and may have a functional role in hepatic lipid homeostasis. MicroRNAs have emerged as important regulators of gene expression post-transcriptionally and in *Gallus gallus* are known to play crucial roles in various biological processes such as the accumulation of abdominal fat⁶⁸ and the lipid metabolism⁶⁹.

In conclusion, the present GWAS revealed a large number of genomic regions and genes implicated in the genetic architecture of a complex trait such as the BW that fully complies with the Fisher's infinitesimal model of inheritance. Exploitation of both community structure and functional enrichment analyses highlighted 3 modules as related to development. Current findings also indicated 52 modular genes participating in developmental processes and 14 more modular genes related to BW. Finally, the present study proposed 66 functional candidate genes for BW, some of which are novel and some identified candidates in previous studies.

Methods

Ethics statement. All animals included in this study were not subjected to any invasive procedures.

Data and quality control. In total, $n = 6,727$ broilers ($n = 3,735$ males and $n = 2,992$ females) from a grand-grandparent (GGP) commercial line with records on BW at 35 days of age were made available by Aviagen Ltd. Phenotypic records for BW ranged from 1,130 to 2,630 g with an average of 1840.2 g (SD = 194 g). Animals were genotyped using the 600k Affymetrix® Axiom® high density genotyping array⁴ resulting in a total number of 578,815 SNPs. Only autosomal SNPs ($n = 547,705$) were considered. Quality control was performed first at a sample and second at a marker level. At a sample level, 72 females and 57 males were excluded due to call rate < 0.99 and autosomal heterozygosity outside the 1.5 IQR (inter-quartile range) resulting in a number of $n = 6,598$ samples. At a marker level, a number of 285,717 SNPs were excluded due to: call rate < 0.99 , MAF (minor allele frequency) < 0.01 and linkage disequilibrium (LD) r^2 values greater than 0.99 within windows of 1 Mb inter-marker distance(s). A total of 6,598 samples and 262,067 SNPs were retained for GWAS. Quality control was performed using the SNP & Variation Suite software (version 8.8.1) of Golden Helix (<http://www.goldenhelix.com>).

Statistical analysis. A multi-locus mixed-model (MLMM) stepwise regression with forward inclusion and backward elimination⁷⁰ of SNPs was employed to identify genome-wide significant markers associated with the trait. The following statistical model was applied to the data:

$$y = X\beta + w\alpha + Z\mathbf{u} + e$$

where y is the $n \times 1$ vector of phenotypic values of BW for n broilers, X is the $n \times 55$ matrix of fixed effects: sex (2 classes), hatch (36 classes) and mating group (17 classes), β is the 55×1 vector of corresponding coefficients of fixed effects, w is the vector with elements of 0, 1, and 2 for the homozygote of the minor allele, heterozygote, and homozygote of the major allele, α is the vector of the fixed effect for the minor allele of the candidate SNP to be tested for association, Z is the incidence matrix relating observations to the polygenic random effects, \mathbf{u} is the vector of polygenic random effects and e is the vector of random residuals.

The random effects were assumed to be normally distributed with zero means and the following covariance structure:

$$\text{Var}\begin{bmatrix} \mathbf{u} \\ e \end{bmatrix} = \begin{bmatrix} G\sigma_u^2 & 0 \\ 0 & I\sigma_e^2 \end{bmatrix}$$

where σ_u^2 and σ_e^2 are the polygenic and error variance components, I is the $n \times n$ identity matrix, and G is the $n \times n$ genomic relationship matrix (GRM⁷¹) with elements of pairwise relationship coefficient using the 262,067 SNPs. The genomic relationship coefficient between two individuals j and k , was estimated as follows:

$$\frac{1}{262,067} \sum_{i=1}^{262,067} \frac{(x_{ij} - 2p_i)(x_{ik} - 2p_i)}{2p_i(1 - 2p_i)}$$

where x_{ij} and x_{ik} represent the number (0, 1, or 2) of the minor allele for the i_{th} SNP of the j_{th} and k_{th} individuals, and p_i is the frequency of the minor allele⁷¹.

Statistically significant markers were selected at the optimal step of the MLM stepwise regression according to extended Bayesian Information Criterion (eBIC⁷²). P-values of these SNPs were then corrected for multiple comparisons using the false-discovery rate (FDR⁷³) correction method. Here, a cut-off FDR p-value less than 0.05⁷⁴ was considered as significant. The FDR p-value of 0.05 states that, among all observed results, 5% would be false positives.

A Quantile-quantile (Q-Q) plot was also used to analyze the extent to which the observed distribution of the test statistic followed the expected (null) distribution. This plot along with the estimation of the genomic inflation factor (λ) was done to assess potential systematic bias due to population structure or to the analytical approach²⁸. This analysis was performed using the SNP & Variation Suite (version 8.8.1) software (Golden Helix: <http://www.goldenhelix.com>).

Detection of candidate genomic regions with strong LD. We first estimated LD levels around each lead i.e. significant SNP. We then searched for genomic regions with strong LD around the lead SNPs defined as the maximum distance between the lead and the last SNP with $D' \geq 0.8$ ⁷⁵. Note that, the D' , instead of the r^2 LD measurement, was preferably used here as the first one is reported to be independent⁷⁶ or less dependent⁷⁷ on MAF. All LD calculations were performed using the SNP & Variation Suite (version 8.8.1) software (Golden Helix: <http://www.goldenhelix.com>).

Identification of reported QTL and positional candidate genes. Next, we searched for growth/fatness related QTL in the ChickenQTLdb¹ and positional candidate genes in the NCBI database^{78,79}, within the strong LD genomic regions. Positions of QTL were remapped from *Gallus gallus* 4 to *Gallus gallus*-5.0 assembly using the Genome Remapping Service from NCBI database⁸⁰.

Detection of community structure and functional module characterization. A gene network using all positional candidate genes was first constructed integrating the available *Homo sapiens* genes database (updated 17/3/2017) via the GeneMANIA V.3.4.1 plug-in¹¹ in Cytoscape V3.6.0 (<http://cytoscape.org>)⁸¹. The gene network was built according to 7 types of interaction terms i.e. co-expression, co-localization, genetic interaction, pathway, physical interaction, predicted and shared protein domains. The automatic weighting method for network construction was also used while the number of related genes was set to zero.

Detection of community structure i.e. the appearance of densely interconnected nodes (modules) was then performed using the Girvan and Newman's clustering algorithm²⁹ via the GLay⁸² of clusterMaker⁸³ plugin in Cytoscape⁸¹. This algorithm identifies modules within networks by repetitively removing edges with the highest "betweenness" i.e. edges between modules with higher values of betweenness rather than edges within modules. The strength of the network division into modules was also quantified using the modularity measure²⁹. Typically, modularity values ranging from 0.3 to 0.7 are indicative of strong community structure²⁹.

Modular genes were then subjected to GO Biological Process (BP) term enrichment analysis using the DAVID functional annotation tool (<https://david.ncifcrf.gov/>, version 6.8)⁸⁴. The *Homo sapiens* species was also selected for the input gene list and as whole genome background for enrichment analysis. The following settings were used during this analysis: an EASE score (a modified Fisher exact p-value⁸⁵) cut-off = 0.05 and a minimum number of genes per GO BP term = 2. GO biological processes with p-values lower than 0.05 were considered as significantly enriched. The QuickGO⁸⁶ web-based tool was subsequently used to examine each resulting significantly enriched GO BP through browsing the hierarchical structure in the GO annotation database. GO BPs associated with developmental process or growth parent term(s) were considered as functionally relevant to the trait under study.

Data Availability

The data that support the findings of this study are available from Aviagen Ltd. but restrictions apply to the availability of these data, which were used under license for the current study, and so are not publicly available. Data are however available from the authors upon reasonable request and with permission of Aviagen Ltd.

References

1. Chicken QTL Database. Available at: <https://www.animalgenome.org/cgi-bin/QTLdb/GG/download?tmpname=mapDwnLd&file=cM>. (Accessed: 3rd September 2017).
2. Xie, L. *et al.* Genome-Wide Association Study Identified a Narrow Chromosome 1 Region Associated with Chicken Growth Traits. *PLoS One* **7**, e30910 (2012).
3. Van Goor, A. *et al.* Identification of quantitative trait loci for body temperature, body weight, breast yield, and digestibility in an advanced intercross line of chickens under heat stress. *Genet. Sel. Evol.* **47**, 96 (2015).
4. Kranis, A. *et al.* Development of a high density 600K SNP genotyping array for chicken. *BMC Genomics* **14**, 59 (2013).
5. Pettersson, M. E. & Carlborg, Ö. Dissecting the genetic architecture of complex traits and its impact on genetic improvement programs: lessons learnt from the Virginia chicken lines. *Rev. Bras. Zootec.* **39**, 256–260 (2010).
6. Shahjahan, M. *et al.* Identification of Histone Deacetylase 2 as a Functional Gene for Skeletal Muscle Development in Chickens. *Asian-Australasian J. Anim. Sci.* **29**, 479–486 (2016).
7. Ouyang, H. *et al.* Identification, expression and variation of the *GNPDA2* gene, and its association with body weight and fatness traits in chicken. *PeerJ* **4**, e2129 (2016).
8. Subramanian, A. *et al.* Gene set enrichment analysis: a knowledge-based approach for interpreting genome-wide expression profiles. *Proc. Natl. Acad. Sci. USA* **102**, 15545–50 (2005).
9. García-Campos, M. A., Espinal-Enríquez, J. & Hernández-Lemus, E. Pathway Analysis: State of the Art. *Front. Physiol.* **6**, 383 (2015).
10. Chen, J., Aronow, B. J. & Jegga, A. G. Disease candidate gene identification and prioritization using protein interaction networks. *BMC Bioinformatics* **10**, 73 (2009).
11. Montojo, J. *et al.* GeneMANIA Cytoscape plugin: fast gene function predictions on the desktop. *Bioinformatics* **26**, 2927–2928 (2010).
12. Walker, M. G., Volkmut, W., Sprinzak, E., Hodgson, D. & Klingler, T. Prediction of gene function by genome-scale expression analysis: prostate cancer-associated genes. *Genome Res.* **9**, 1198–203 (1999).
13. Oliver, S. Guilt-by-association goes global. *Nature* **403**, 601–602 (2000).
14. Liu, G., Wang, H., Chu, H., Yu, J. & Zhou, X. Functional diversity of topological modules in human protein-protein interaction networks. *Sci. Rep.* **7**, 16199 (2017).
15. Terentiev, A. A., Moldogazieva, N. T. & Shaitan, K. V. Dynamic proteomics in modeling of the living cell. Protein-protein interactions. *Biochemistry. (Mosc.)* **74**, 1586–607 (2009).
16. Spirin, V. & Mirny, L. A. Protein complexes and functional modules in molecular networks. *Proc. Natl. Acad. Sci. USA* **100**, 12123–8 (2003).
17. Lu, H. *et al.* Integrated analysis of multiple data sources reveals modular structure of biological networks. *Biochem. Biophys. Res. Commun.* **345**, 302–309 (2006).
18. Zhang, S., Ning, X. & Zhang, X.-S. Identification of functional modules in a PPI network by clique percolation clustering. *Comput. Biol. Chem.* **30**, 445–451 (2006).
19. Sharan, R., Ulitsky, I. & Shamir, R. Network-based prediction of protein function. *Mol. Syst. Biol.* **3**, 88 (2007).
20. Jagannadham, J., Jaiswal, H. K., Agrawal, S. & Rawal, K. Comprehensive Map of Molecules Implicated in Obesity. *PLoS One* **11**, e0146759 (2016).
21. Sharma, P., Bhattacharyya, D. K. & Kalita, J. Disease biomarker identification from gene network modules for metastasized breast cancer. *Sci. Rep.* **7**, 1072 (2017).
22. Hallett, R. M. *et al.* Identification and evaluation of network modules for the prognosis of basal-like breast cancer. *Oncotarget* **6**, 17713–24 (2015).
23. Lempiäinen, H. *et al.* Network analysis of coronary artery disease risk genes elucidates disease mechanisms and druggable targets. *Sci. Rep.* **8**, 3434 (2018).
24. Sharma, A. *et al.* A disease module in the interactome explains disease heterogeneity, drug response and captures novel pathways and genes in asthma. *Hum. Mol. Genet.* **24**, 3005–3020 (2015).
25. Hira, R., Terada, S.-I., Kondo, M. & Matsuzaki, M. Distinct Functional Modules for Discrete and Rhythmic Forelimb Movements in the Mouse Motor Cortex. *J. Neurosci.* **35**, 13311–13322 (2015).
26. Liu, J. *et al.* Protein Profiles for Muscle Development and Intramuscular Fat Accumulation at Different Post-Hatching Ages in Chickens. *PLoS One* **11**, e0159722 (2016).
27. Kang, H. M. *et al.* Variance component model to account for sample structure in genome-wide association studies. *Nat. Genet.* **42**, 348–354 (2010).
28. Yang, J. *et al.* Genomic inflation factors under polygenic inheritance. *Eur. J. Hum. Genet.* **19**, 807–12 (2011).
29. Newman, M. E. J. & Girvan, M. Finding and evaluating community structure in networks. *Phys. Rev. E* **69**, 026113 (2004).
30. Kamaid, A. & Giráldez, F. *Btg1* and *Btg2* gene expression during early chick development. *Dev. Dyn.* **237**, 2158–2169 (2008).
31. Sun, C. *et al.* Promising Loci and Genes for Yolk and Ovary Weight in Chickens Revealed by a Genome-Wide Association Study. *PLoS One* **10**, e0137145 (2015).
32. Reijntjes, S., Stricker, S. & Mankoo, B. S. A comparative analysis of *Meox1* and *Meox2* in the developing somites and limbs of the chick embryo. *Int. J. Dev. Biol.* **51**, 753–759 (2007).
33. Couteaudier, M. *et al.* Derivation of keratinocytes from chicken embryonic stem cells: Establishment and characterization of differentiated proliferative cell populations. *Stem Cell Res.* **14**, 224–237 (2015).
34. Tarique, T. *et al.* Identification of genes involved in regulatory mechanism of pigments in broiler chickens. *Genet. Mol. Res.* **13**, 7201–7216 (2014).
35. Gu, X. *et al.* Genome-Wide Association Study of Body Weight in Chicken F2 Resource Population. *PLoS One* **6**, e21872 (2011).
36. Gibson, M. S., Kaiser, P. & Fife, M. Identification of Chicken Granulocyte Colony-Stimulating Factor (G-CSF/CSF3): The Previously Described Myelomonocytic Growth Factor Is Actually CSF3. *J. Interf. Cytokine Res.* **29**, 339–344 (2009).
37. Bou-Gharios, G., Liu, K., Li, I. & De Val, S. Three new functionally conserved cis-regulatory elements in the *Acan* gene. *Osteoarthritis Cartil.* **22**, S143–S144 (2014).
38. Gouveia, A., Marcelino, H. M., Gonçalves, L., Palmeirim, I. & Andrade, R. P. Patterning in time and space: *HoxB* cluster gene expression in the developing chick embryo. *Cell Cycle* **14**, 135 (2015).
39. Li, J. *et al.* DNA methylation of *CMTM3*, *SSTR2*, and *MDF1* genes in colorectal cancer. *Gene* **630**, 1–7 (2017).
40. Suzuki, S., Namiki, J., Shibata, S., Mastuzaki, Y. & Okano, H. The Neural Stem/Progenitor Cell Marker Nestin Is Expressed in Proliferative Endothelial Cells, but Not in Mature Vasculature. *J. Histochem. Cytochem.* **58**, 721–730 (2010).
41. Maridas, D. E., DeMambro, V. E., Le, P. T., Mohan, S. & Rosen, C. J. *IGFBP4* Is Required for Adipogenesis and Influences the Distribution of Adipose Depots. *Endocrinology* **158**, 3488–3500 (2017).

42. Rucci, N. *et al.* The glycosaminoglycan-binding domain of PRELP acts as a cell type-specific NF-kappaB inhibitor that impairs osteoclastogenesis. *J. Cell Biol.* **187**, 669–83 (2009).
43. Shue, Y.-L., Chen, L.-R., Tsai, C.-J., Yeh, C.-Y. & Huang, C.-T. Emerging roles of peroxisome proliferator-activated receptors in the pituitary gland in female reproduction. *Biomarkers Genomic Med.* **5**, 1–11 (2013).
44. Guan, F. H. X. *et al.* The antiproliferative ELF2 isoform, ELF2B, induces apoptosis *in vitro* and perturbs early lymphocytic development *in vivo*. *J. Hematol. Oncol.* **10**, 75 (2017).
45. Sen, R. *et al.* Kat2a and Kat2b Acetyltransferase Activity Regulates Craniofacial Cartilage and Bone Differentiation in Zebrafish and Mice. *J. Dev. Biol.* **6**, 27 (2018).
46. Huang, H. *et al.* Changes in the expression and subcellular localization of RAR α in the rat hippocampus during postnatal development. *Brain Res.* **1227**, 26–33 (2008).
47. Jiang, S., Cheng, H. W., Hester, P. Y. & Hou, J.-F. Development of an enzyme-linked immunosorbent assay for detection of chicken osteocalcin and its use in evaluation of perch effects on bone remodeling in caged White Leghorns. *Poult. Sci.* **92**, 1951–1961 (2013).
48. Manca, A. *et al.* Nerve growth factor regulates axial rotation during early stages of chick embryo development. *Proc. Natl. Acad. Sci.* **109**, 2009–2014 (2012).
49. Li, J. *et al.* APOBEC2 mRNA and protein is predominantly expressed in skeletal and cardiac muscles of chickens. *Gene* **539**, 263–269 (2014).
50. Zhao, X. H. *et al.* Single nucleotide polymorphism in the STAT5b gene is associated with body weight and reproductive traits of the Jinghai Yellow chicken. *Mol. Biol. Rep.* **39**, 4177–4183 (2012).
51. Johnston, P. A. & Grandis, J. R. STAT3 SIGNALING: Anticancer Strategies and Challenges. *Mol. Interv.* **11**, 18–26 (2011).
52. Zhao, M., Mishra, L. & Deng, C.-X. The role of TGF- β /SMAD4 signaling in cancer. *Int. J. Biol. Sci.* **14**, 111–123 (2018).
53. Hasegawa, N. *et al.* Mediator Subunits MED1 and MED24 Cooperatively Contribute to Pubertal Mammary Gland Development and Growth of Breast Carcinoma Cells. *Mol. Cell. Biol.* **32**, 1483–1495 (2012).
54. Chen, F. *et al.* Neuromuscular synaptic patterning requires the function of skeletal muscle dihydropyridine receptors. *Nat. Neurosci.* **14**, 570–577 (2011).
55. van der Vaart, B. *et al.* SLAIN2 links microtubule plus end-tracking proteins and controls microtubule growth in interphase. *J. Cell Biol.* **193**, 1083–1099 (2011).
56. Brachner, A., Reipert, S., Foisner, R. & Gotzmann, J. LEM2 is a novel MAN1-related inner nuclear membrane protein associated with A-type lamins. *J. Cell Sci.* **118**, 5797–810 (2005).
57. Tapia, O., Fong, L. G., Huber, M. D., Young, S. G. & Gerace, L. Nuclear Envelope Protein Lem2 is Required for Mouse Development and Regulates MAP and AKT Kinases. *PLoS One* **10**, e0116196 (2015).
58. Giacometti, S. *et al.* Mutually Exclusive CBC-Containing Complexes Contribute to RNA Fate. *Cell Rep.* **18**, 2635–2650 (2017).
59. Winczura, K. *et al.* Characterizing ZC3H18, a Multi-domain Protein at the Interface of RNA Production and Destruction Decisions. *Cell Rep.* **22**, 44–58 (2018).
60. Iwakawa, R. *et al.* Expression and clinical significance of genes frequently mutated in small cell lung cancers defined by whole exome/RNA sequencing. *Carcinogenesis* **36**, 616–621 (2015).
61. Zhang, G. X. *et al.* Genome-wide association study of growth traits in the Jinghai Yellow chicken. *Genet. Mol. Res.* **14**, 15331–15338 (2015).
62. Pampouille, E. *et al.* Mapping QTL for white striping in relation to breast muscle yield and meat quality traits in broiler chickens. *BMC Genomics* **19**, 202 (2018).
63. Sun, D., Liu, Y., Zhang, X.-S. & Wu, L.-Y. CEA: Combination-based gene set functional enrichment analysis. *Sci. Rep.* **8**, 13085 (2018).
64. Tarsani, E., Kranis, A., Maniatis, G. & Kominakis, A. Investigating the functional role of 1,012 candidate genes identified by a Genome Wide Association Study for body weight in broilers. *Proc. World Congr. Genet. Appl. to Livest. Prod. Species-Avian 1*, 564 (2018).
65. Yuan, J. *et al.* Genome-wide association studies for feed intake and efficiency in two laying periods of chickens. *Genet. Sel. Evol.* **47**, 82 (2015).
66. Jiajie, T., Yanzhou, Y., Hoi-Hung, A. C., Zi-Jiang, C. & Wai-Yee, C. Conserved miR-10 family represses proliferation and induces apoptosis in ovarian granulosa cells. *Sci. Rep.* **7**, 41304 (2017).
67. Singaravelu, R. *et al.* MicroRNA-7 mediates cross-talk between metabolic signaling pathways in the liver. *Sci. Rep.* **8**, 361 (2018).
68. Huang, H. Y. *et al.* Integrated analysis of microRNA and mRNA expression profiles in abdominal adipose tissues in chickens. *Sci. Rep.* **5**, 16132 (2015).
69. Li, H. *et al.* Systematic analysis of the regulatory functions of microRNAs in chicken hepatic lipid metabolism. *Sci. Rep.* **6**, 31766 (2016).
70. Segura, V. *et al.* An efficient multi-locus mixed-model approach for genome-wide association studies in structured populations. *Nat. Genet.* **44**, 825–830 (2012).
71. VanRaden, P. M. Efficient Methods to Compute Genomic Predictions. *J. Dairy Sci.* **91**, 4414–4423 (2008).
72. Chen, J. & Chen, Z. Extended Bayesian information criteria for model selection with large model spaces. *Biometrika* **95**, 759–771 (2008).
73. Benjamini, Y. & Hochberg, Y. Controlling the False Discovery Rate: A Practical and Powerful Approach to Multiple Testing. *Journal of the Royal Statistical Society. Series B (Methodological)* **57**, 289–300 (1995).
74. Qu, H.-Q., Tien, M. & Polychronakos, C. Statistical significance in genetic association studies. *Clin. Invest. Med.* **33**, E266–70 (2010).
75. Yi, G. *et al.* Genome-wide association study dissects genetic architecture underlying longitudinal egg weights in chickens. *BMC Genomics* **16**, 746 (2015).
76. Hedrick, P. W. Gametic disequilibrium measures: proceed with caution. *Genetics* **117**, 331–41 (1987).
77. McRae, A. F. *et al.* Linkage disequilibrium in domestic sheep. *Genetics* **160**, 1113–22 (2002).
78. Gallus gallus Annotation Release 103. Available at: https://www.ncbi.nlm.nih.gov/genome/annotation_euk/Gallus_gallus/103/. (Accessed: 3rd September 2017).
79. Gallus_gallus-5.0 in NCBI assembly data base. Available at: https://www.ncbi.nlm.nih.gov/assembly/GCF_000002315.4/. (Accessed: 3rd September 2017)
80. Coordinate remapping service: NCBI. Available at: <https://www.ncbi.nlm.nih.gov/genome/tools/remap>. (Accessed: 3rd September 2017)
81. Shannon, P. *et al.* Cytoscape: A Software Environment for Integrated Models of Biomolecular Interaction Networks. *Genome Res.* **13**, (2498–2504) (2003).
82. Su, G., Kuchinsky, A., Morris, J. H., States, D. J. & Meng, F. GLayer: community structure analysis of biological networks. *Bioinformatics* **26**, 3135–3137 (2010).
83. Morris, J. H. *et al.* clusterMaker: a multi-algorithm clustering plugin for Cytoscape. *BMC Bioinformatics* **12**, 436 (2011).
84. Dennis, G. *et al.* DAVID: Database for Annotation, Visualization, and Integrated Discovery. *Genome Biol.* **4**, R60 (2003).
85. Hosack, D. A. *et al.* Identifying biological themes within lists of genes with EASE. *Genome Biol.* **4**, R70 (2003).
86. Huntley, R. P. *et al.* QuickGO: a user tutorial for the web-based Gene Ontology browser. *Database (Oxford)*. **2009**, bap010 (2009).
87. Conant, G. C. & Wolfe, K. H. GenomeVx: simple web-based creation of editable circular chromosome maps. *Bioinformatics* **24**, 861–862 (2008).

Author Contributions

E.T. performed all the analyses and drafted the main manuscript text. A.K.R., G.M. and S.A. conducted data collection and preparation and contributed to writing the manuscript. A.L.H.T. assisted in the search and identification of Q.T.L. and candidate genes and contributed to writing the manuscript. A.K. conceived and supervised the study and drafted the final version of the manuscript. All authors read and approved the final manuscript.

Additional Information

Supplementary information accompanies this paper at <https://doi.org/10.1038/s41598-019-45520-5>.

Competing Interests: The authors declare no competing interests.

Publisher's note: Springer Nature remains neutral with regard to jurisdictional claims in published maps and institutional affiliations.



Open Access This article is licensed under a Creative Commons Attribution 4.0 International License, which permits use, sharing, adaptation, distribution and reproduction in any medium or format, as long as you give appropriate credit to the original author(s) and the source, provide a link to the Creative Commons license, and indicate if changes were made. The images or other third party material in this article are included in the article's Creative Commons license, unless indicated otherwise in a credit line to the material. If material is not included in the article's Creative Commons license and your intended use is not permitted by statutory regulation or exceeds the permitted use, you will need to obtain permission directly from the copyright holder. To view a copy of this license, visit <http://creativecommons.org/licenses/by/4.0/>.

© The Author(s) 2019